INTERNATIONAL JOURNAL FOR NUMERICAL METHODS IN FLUIDS, VOL. 12, 881–894 (1991)

DYNAMICS OF LIQUID MEMBRANES. II: ADAPTIVE FINITE DIFFERENCE METHODS

J. I. RAMOS*

F. Informática/E.T.S.I. Telecomunicación, Universidad de Málaga, Plaza El Ejido, E-29013-Málaga, Spain

SUMMARY

Two domain-adaptive finite difference methods are presented and applied to study the dynamic response of incompressible, inviscid, axisymmetric liquid membranes subject to imposed sinusoidal pressure oscillations. Both finite difference methods map the time-dependent physical domain whose downstream boundary is unknown onto a fixed computational domain. The location of the unknown time-dependent downstream boundary of the physical domain is determined from the continuity equation and results in an integrodifferential equation which is non-linearly coupled with the partial differential equations which govern the conservation of mass and linear momentum and the radius of the liquid membrane. One of the finite difference methods solves the non-conservative form of the governing equations by means of a block implicit iterative method. This method possesses the property that the Jacobian matrix of the convection fluxes has an eigenvalue of algebraic multiplicity equal to four and of geometric multiplicity equal to one. The second finite difference procedure also uses a block implicit iterative method, but the governing equations are written in conservation law form and contain an axial velocity which is the difference between the physical axial velocity and the grid speed. It is shown that these methods yield almost identical results and are more accurate than the non-adaptive techniques presented in Part I. It is also shown that the actual value of the pressure coefficient determined from linear analyses can be exceeded without affecting the stability and convergence of liquid membranes if the liquid membranes are subjected to sinusoidal pressure variations of sufficiently high frequencies.

KEY WORDS Liquid membranes Adaptive finite difference methods Integrodifferential equations

INTRODUCTION

In Part I[1] a non-adaptive procedure and a Lagrangian–Eulerian formulation were used to study the dynamic response of incompressible, inviscid, axisymmetric liquid membranes subject to imposed step and ramp changes in the pressure coefficient.

It was shown in Part I that non-adaptive methods require that the largest convergence length of the liquid membrane be known before its dynamic response can be studied. It was also shown that the largest convergence length must correspond to the largest imposed pressure coefficient and that some grid points are never used in the calculations if non-adaptive grids are used to study the dynamics of liquid membranes.

In this paper two adaptive finite difference methods are developed and applied to study the dynamic response of liquid membranes subject to imposed sinusoidal pressure fluctuations. These methods map the physical domain defined as the distance between the nozzle exit and the liquid

* On leave from Department of Mechanical Engineering, Carnegie-Mellon University, Pittsburgh, PA 15213-3890, U.S.A.

0271–2091/91/090881–14$07.00 *Received 4 September 1989*

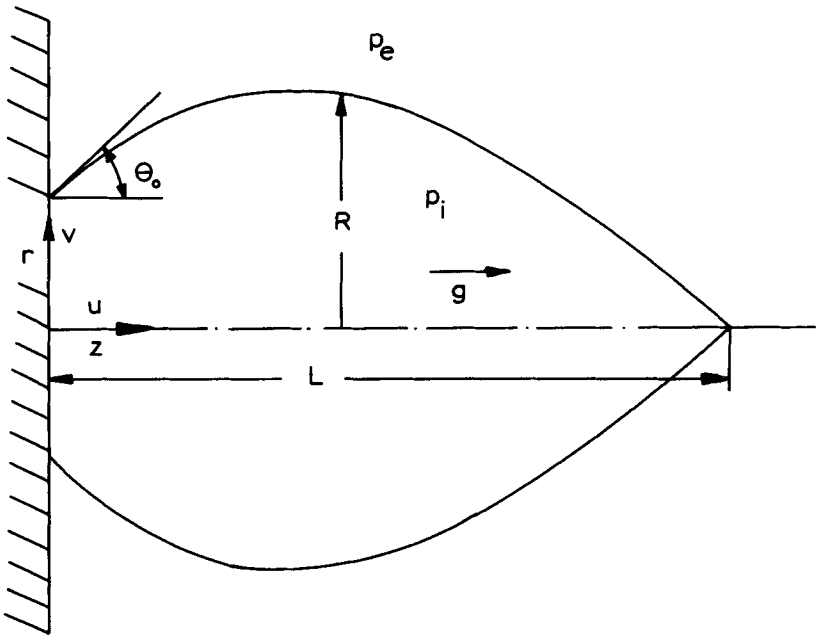

Figure 1. Schematic of a liquid membrane

membrane convergence point (Figure 1) onto a fixed computational domain. This mapping automatically ensures that all the grid points are employed in the calculations; however, the time-dependent convergence length of the liquid membrane is unknown and must be determined as part of the solution.

By appropriate integrations of the continuity equation from the nozzle exit to the liquid membrane convergence point, an integrodifferential equation for the convergence length can be derived. This integrodifferential equation contains the axial velocity and the mass (per unit length and per radian) of the liquid membrane at the convergence point and the total mass (per radian) of the liquid membrane; it is therefore non-linearly coupled with the four partial differential equations which govern the radius and the conservation of mass and linear momentum of the liquid membrane. This means that the adaptive finite difference methods presented in this paper require the solution of *five* differential equations as compared with the *four* differential equations solved by the non-adaptive procedures presented in Part I.

Ramos[2] has shown that for steady state liquid membranes exiting the nozzle with zero angle, there is a critical value of the pressure coefficient C_{pn}, beyond which the liquid membrane is either a cylindrical surface or never converges. It will be shown in this paper that the critical value of the steady state pressure coefficient determined from linear analyses can be exceeded if the liquid membrane is subjected to sinusoidal pressure fluctuations of sufficiently high frequency. These high frequencies result in oscillating membranes whose stability and response depend on the amplitude and frequency of the imposed pressure fluctuations and on the Froude number, convergence parameter and nozzle exit angle.

The results of the adaptive finite difference methods presented in this paper are also compared with the non-adaptive techniques of Part I in order to assess their accuracy and efficiency in the

computation of the dynamic response of liquid membranes subject to imposed sinusoidal pressure oscillations.

PROBLEM FORMULATION

The non-dimensional equations governing the dynamics of isothermal, inviscid, axisymmetric curtains have been presented in Part I.[1] For the sake of convenience these equations are written as

$$\frac{\partial \mathbf{U}}{\partial \tau}+\frac{\partial \mathbf{F}}{\partial z^*}=\mathbf{G} \qquad (\tau>0,\ 0<z^*\leq L^*(\tau)), \tag{1}$$

where

$$\mathbf{U}=(m^*, R_1^*, M^*, N^*)^{\mathrm{T}}, \tag{2}$$

$$\mathbf{F}=[M^*, R_1^* M^*/m^*, M^{*2}/m^*, M^* N^*/m^*]^{\mathrm{T}}, \tag{3}$$

$$\mathbf{G}=[0, N^*, Fr\ m^*-(C_{\mathrm{pn}} R^* R^{*\prime}-J^{*\prime})/N, (-J^{*\prime}/R^{*\prime}+C_{\mathrm{pn}} R^*)/N]^{\mathrm{T}}, \tag{4}$$

$$J^*=R^*\Big/\left[1+\left(\frac{\partial R^*}{\partial z^*}\right)^2\right]^{1/2}, \tag{5}$$

$$C_{\mathrm{pn}}=(p_{\mathrm{i}}-p_{\mathrm{e}})\frac{R_0}{2\sigma}, \qquad Fr=\frac{u_0^2}{gR_0}, \qquad We=\frac{m_0 u_0^2}{2\sigma R_0}, \qquad N=\frac{We}{Fr^2}, \tag{6}$$

$$M^*=m^* u^*, \qquad N^*=m^* v^*, \qquad R_1^*=m^* R^*. \tag{7}$$

Here τ and z^* denote the non-dimensional time and non-dimensional axial co-ordinate respectively, m^* is the non-dimensional mass per unit length and per radian, M^* and N^* denote the axial and radial momentum components per unit length and per radian respectively, Fr and We are the Froude and Weber numbers respectively, N is the convergence parameter, u^* and v^* denote the liquid membrane non-dimensional axial and radial velocity components respectively, R^* is the non-dimensional radius, the primes denote differentiation with respect to z^*, C_{pn} is the pressure coefficient, p_{i} and p_{e} are the pressures of the gases enclosed by and surrounding the liquid membrane respectively, σ is the surface tension, g is the gravitational acceleration, R_0, u_0 and m_0 denote the (dimensional) radius, axial velocity component and mass of the liquid membrane per unit length and per radian at the nozzle exit respectively, the superscript T denotes transpose and L^* denotes the liquid membrane convergence length, i.e. the axial location at which $R^*(\tau, L^*)=0$.

Equation (1) is subjected to the following boundary condition at the nozzle exit:

$$\mathbf{U}(\tau, 0)=[1, 1, 1, \tan\theta_0]^{\mathrm{T}}, \tag{8}$$

where θ_0 denotes the nozzle exit angle (Figure 1).

In this paper we study the dynamic response of liquid membranes to imposed pressure fluctuations, i.e. to $C_{\mathrm{pn}}=C_{\mathrm{pn}}(\tau)$. The mixed convection–diffusion problem represented by equation (1) is such that the solution of equation (1) must be obtained in the domain $0<z^*<L^*(\tau)$, i.e. from the nozzle exit to the convergence of the liquid membrane. However, the convergence length $L^*(\tau)$ is not known in advance and must be determined as part of the solution.

It was shown in Part I that $L^*(\tau)$ can be determined using non-adaptive and Lagrangian–Eulerian finite difference procedures. However, these methods require that the largest value of L^*, i.e. $L^*_{\max}$, be known before the solution of equation (1) is obtained. Furthermore, the solution of equation (1) in fixed (non-adaptive) grids implies that the grid points located in the interval $L^*(\tau)\leq z^*\leq L^*_{\max}$ are never used in the calculations.

In this paper we develop solution-adaptive methods for equation (1) as shown in the next section.

ADAPTIVE METHODS

The following domain-adaptive finite difference methods were used to solve equation (1).

First method

The domain $0 \leq z^* \leq L^*(\tau)$ can be transformed into a fixed one by means of the mapping

$$(\tau, z^*) \rightarrow (\xi, \eta), \tag{9}$$

where

$$\xi = \tau, \qquad \eta = z^*/L^*(\tau), \tag{10}$$

so that $\xi > 0$, $0 \leq \eta \leq 1$ and

$$\frac{\partial}{\partial \tau} = \frac{\partial}{\partial \xi} - \frac{\eta}{L^*}\frac{\mathrm{d}L^*}{\mathrm{d}\tau}\frac{\partial}{\partial \eta}, \qquad \frac{\partial}{\partial z^*} = \frac{1}{L^*}\frac{\partial}{\partial \eta}. \tag{11}$$

Substitution of equation (11) into equation (1) yields

$$\frac{\partial \mathbf{U}}{\partial \xi} + \mathbf{H}_1 \frac{\partial \mathbf{U}}{\partial \eta} = \mathbf{G}, \tag{12}$$

where

$$\mathbf{H}_1 = \frac{1}{L^*}\left(\mathbf{H} - \eta \frac{\mathrm{d}L^*}{\mathrm{d}\tau}\mathbf{I}\right), \tag{13}$$

with

$$\mathbf{H} = \frac{\partial \mathbf{F}}{\partial \mathbf{U}} \tag{14}$$

and $\mathbf{I}$ the unit matrix.

Equation (13) has the same form as equation (16) of Part I and can be solved by means of a block implicit iterative technique.[1] Note that the eigenvalue of $\mathbf{H}_1$ is

$$\lambda = \frac{1}{L^*}\left(\frac{M^*}{m^*} - \eta \frac{\mathrm{d}L^*}{\mathrm{d}\tau}\right), \tag{15}$$

which has an algebraic multiplicity of four and a geometric multiplicity of one. Therefore a similarity transformation of $\mathbf{H}_1$ yields a Jordan canonical form which has λ in the main diagonal and ones in the diagonal above the main diagonal.[3] Furthermore, equation (15) can be written as

$$\lambda = \frac{1}{L^*}\left(u^* - \eta \frac{\mathrm{d}L^*}{\mathrm{d}\tau}\right). \tag{16}$$

Since u^* is always greater than $\mathrm{d}L^*/\mathrm{d}\tau$, the eigenvalues given by equation (16) are strictly positive.

It must be noted that $u^*(\tau, L^*) \neq \mathrm{d}L^*/\mathrm{d}\tau$ since u^* represents the axial velocity of the liquid membrane whereas $\mathrm{d}L^*/\mathrm{d}\tau$ is the velocity at which the convergence point (Figure 1) moves.

Analytical solutions of steady state liquid membranes[2] indicate that u^* is proportional to the Froude number and, since $0 \leq \eta \leq 1$, $\lambda > 0$. This allows one to discretize equation (11) by means of backward differences for the time derivatives, upwind differences for the convection terms and central differences for $\mathbf{G}$. The resulting $O(\Delta\xi, \Delta\eta)$-accurate finite difference equation for (12) can

be written as[1]

$$-\mathbf{C}_i^{n+1}\mathbf{U}_{i-1}^{n+1}+(\mathbf{I}+\mathbf{C}_i^{n+1})\mathbf{U}_i^{n+1}=\Delta\xi\mathbf{G}_i^{n+1}+\mathbf{U}_i^n, \tag{17}$$

where

$$\mathbf{C}=\mathbf{H}_1\Delta\xi/\Delta\eta. \tag{18}$$

Equation (18) represents a block bidiagonal system which can be solved by forward substitution in the following block iterative manner. The value of $\mathbf{U}_i^{n+1}$ was guessed and used to evaluate $\mathbf{G}_i^{n+1}$. Equation (18) was then solved and the value of $\mathbf{U}_i^{n+1}$ was updated until

$$\left(\sum_{i=1}^{N_P}(\mathbf{U}_i^{*k+1}-\mathbf{U}_i^{*k})^2\right)^{1/2}\leq 10^{-4}, \tag{19}$$

where N_P denotes the number of grid points used in the calculations, the superscript k denotes the kth iteration within the time step and the subscript i denotes the ith grid point, i.e. $\eta_i=i\Delta\eta$, where $\Delta\eta$ is the spatial step size. Note that

$$(\mathbf{U}_i^{*k+1}-\mathbf{U}_i^{*k})^2=(\mathbf{U}_i^{*k+1}-\mathbf{U}_i^{*k})^{\mathrm{T}}(\mathbf{U}_i^{*k+1}-\mathbf{U}_i^{*k}).$$

The block implicit procedure just described can easily be implemented in a computer programme; however, the value of L^* which appears in equation (13) remains as yet unspecified and a procedure must be devised to calculate it.

The value of L^* can be calculated from any of the four equations represented in (1). For example, consider the first component of equation (1), i.e.

$$\frac{\partial m^*}{\partial\tau}+\frac{\partial}{\partial z^*}(m^*u^*)=0, \tag{20}$$

which represents the continuity equation. Equation (20) can be integrated from the nozzle exit ($z^*=0$) to the unknown convergence point ($z^*=L^*(\tau)$) to yield, after application of Leibnitz's rule,

$$\frac{\mathrm{d}L^*}{\mathrm{d}\tau}=\frac{1}{m^*(\tau,L^*)}\left(\frac{\mathrm{d}}{\mathrm{d}\tau}\int_0^{L^*}m^*\mathrm{d}z^*+m^*(\tau,L^*)u^*(\tau,L^*)-1\right), \tag{21}$$

since $m^*(\tau,0)=u^*(\tau,0)=1$ at the nozzle exit, and the integral one the right-hand side of equation (21) represents the total mass (per radian) of the liquid membrane.

Substitution of equation (10) into equation (21) yields the following integrodifferential equation:

$$\frac{\mathrm{d}L^*}{\mathrm{d}\tau}=\frac{1}{m^*(\xi,\eta=1)}\left[\frac{\mathrm{d}}{\mathrm{d}\tau}\left(L^*\int_0^1 m^*\mathrm{d}\eta\right)+m^*(\xi,\eta=1)u^*(\xi,\eta=1)-1\right], \tag{22}$$

whose solution yields the value of $L^*=L^*(\tau)$. Note that the integral on the right-hand side of equation (22) is only a function of ξ and that $\tau=\xi$ (see equation (10)). Note also that this integral and the values of m^* and u^* can be obtained from the solution of equation (17).

Analogous expressions to equation (22) can be obtained from the third and fourth equations of (1). However, these equations contain complex integrals associated with the right-hand sides of the axial and radial linear momentum components. Note also that the first component of equation (1) can be written as ($R_1^*=m^*R^*$)

$$\frac{\partial}{\partial\tau}(m^*R^*)+\frac{\partial}{\partial z^*}(m^*R^*u^*)=m^*v^*. \tag{23}$$

Integration of equation (23) from $z^*=0$ to $z^*=L^*(\tau)$, application of Leibnitz's rule and use of the condition $R^*(\tau, L^*)=0$ and of the continuity equation (see equation (20)) yield

$$\frac{\partial}{\partial\tau}\int_0^{L^*} m^*R^*\,\mathrm{d}z^*=\int_0^{L^*}\frac{\partial}{\partial\tau}(m^*R^*)\,\mathrm{d}z^*. \tag{24}$$

Second method

The second finite difference method used to solve equation (1) also employs the mapping defined by equations (9)–(11), which can be substituted into equation (1) to yield

$$\frac{\partial\mathbf{V}}{\partial\xi}+\frac{\partial}{\partial\eta}(\bar{\mathbf{u}}^*\mathbf{U})=L^*\mathbf{G}, \tag{25}$$

where

$$\mathbf{V}=L^*\mathbf{U}, \qquad \bar{u}^*=u^*-\eta\frac{\mathrm{d}L^*}{\mathrm{d}\tau} \tag{26}$$

and $\bar{u}^*$ is the relative velocity between the fluid and the 'accordion' grid $\eta=z^*/L^*(\tau)$. Note that $0\leq\eta\leq1$ and that $\bar{u}^*>0$.

Equation (25) can also be written as

$$\frac{\partial\mathbf{V}}{\partial\xi}+\frac{\partial}{\partial\eta}\left(\frac{\bar{u}^*}{L^*}\mathbf{V}\right)=L^*\mathbf{G}, \tag{27}$$

which can be solved by means of a block implicit iterative method with backward differences for the time derivatives, upwind differences for the second term on the left-hand side and central differences for the term $L^*\mathbf{G}$. The accuracy of this method, which is conservative, is $O(\Delta\xi, \Delta\eta)$. Note that the effective convection velocity in equation (27) is $\bar{u}^*$, which is greater than u^* when the liquid membrane contracts, i.e. when $\mathrm{d}L^*/\mathrm{d}\tau<0$.

Once the vector $\mathbf{V}$ is calculated from equation (27), the following operation can be performed to obtain $\mathbf{U}$:

$$\mathbf{U}=\frac{1}{L^*}\mathbf{V}. \tag{28}$$

The finite difference discretization of equation (27) requires the specification of L^*. This value can be calculated from equation (22), which was solved by means of a first-order-accurate backward Euler method, i.e.

$$L^{*(n+1)}=\frac{1}{Q^{n+1,n+1}}\{L^{*(n)}Q^{n+1,n}+\Delta\tau[m^{*(n+1)}(\xi,\eta=1)u^{*(n+1)}(\xi,\eta=1)-1]\}, \tag{29}$$

where

$$Q^{ij}=m^{*(i)}(\xi,\eta=1)-\int_0^1 m^{*(j)}(\xi,\eta)\,\mathrm{d}\eta. \tag{30}$$

PRESENTATION OF RESULTS

The calculations presented in this section were performed with $\Delta\xi=0{\cdot}01$ and used from 300 to 400 grid points in the η-co-ordinate ($0\leq\eta\leq1$). The number of grid points was determined so that the results are grid-independent. The values of the parameters used in the calculations are presented in Table I.

Table I. Values of the parameters used in the calculations

Figure	Fr	N	θ_0 (deg)	C_{pna}	St
2	1	15	0	0	—
4	1	15	0	0·5	Variable
5	1	15	0	0·5	0·1
6	Variable	15	0	0·5	0·1
7	1	Variable	0	0·5	0·1
8	1	15	Variable	0·1	0·1
9	1	15	0	Variable	0·2

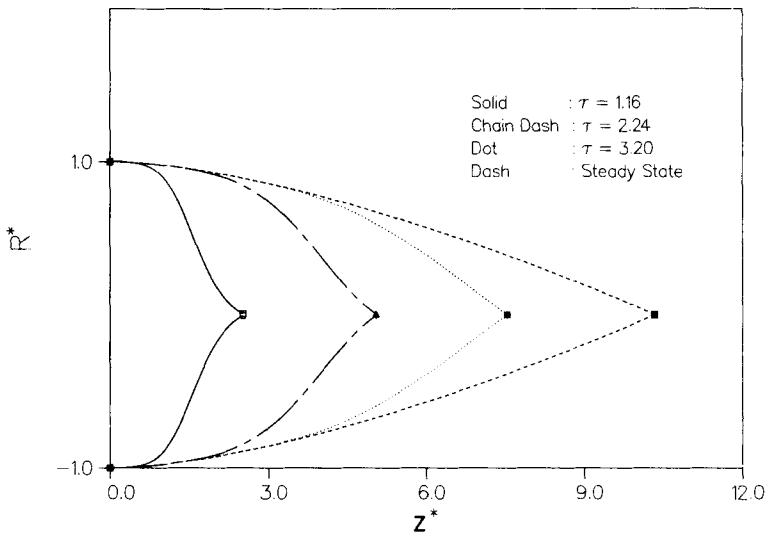

Figure 2. Numerical start-up of a liquid membrane

Figure 2 shows the numerical results corresponding to the start-up of a liquid membrane, i.e. to an initial condition

$$\mathbf{U}(0, \eta) = (0, 0, 0, 0)^{\mathrm{T}}. \tag{31}$$

This numerical start-up of the liquid membrane does not have any connection whatsoever with the physical start-up observed in the laboratory and is presented here to illustrate the robustness of the adaptive finite difference methods presented in this paper. Note that at $\xi = 0^-$ or $\tau = 0^-$ there is no liquid membrane, and that the initial condition of equation (31) is *not mathematically* consistent with the boundary condition of equation (8).

Figure 2 indicates that before the liquid membrane reaches a steady state condition, its profile exhibits a cusp point at the convergence point, i.e. at L^*. A steady state was achieved whenever

$$\left[\sum_{i=1}^{N_P}\left(\frac{\mathbf{U}_i^{n+1} - \mathbf{U}_i^n}{\Delta\xi}\right)^2\right]^{1/2} \leq 10^{-4}, \tag{32}$$

and the convergence length was defined as the axial location at which

$$|R^*| \leq 10^{-4}. \tag{33}$$

Figures 4–9 show the dynamic response of liquid membranes to sinusoidal pressure coefficients such as the one shown schematically in Figure 3. These pressure coefficients can be written as

$$C_{pn} = C_{pna} \sin(2\pi f t), \tag{34}$$

where C_{pna} is the amplitude, $2\pi f$ is the circular frequency and t is dimensional time.

Introducing the following non-dimensional groups (see Part I),

$$St = fR_0/u_0, \qquad \tau = gt/u_0, \tag{35}$$

equation (34) can be written as

$$C_{pn} = C_{pna} \sin(2\pi St Fr \tau), \tag{36}$$

where St is the Strouhal number which represents the ratio of the frequency of the imposed pressure perturbation to a characteristic frequency of the liquid membrane.

In Figures 4–9 the nondimensional convergence length has been normalized by that corresponding to steady state liquid membranes with $C_{pn} = 0$, i.e. with respect to L^*_{ss}.

Figure 4 shows the dynamic response of a liquid membrane to sinusoidal pressure coefficients whose amplitude C_{pna} is kept constant while the frequency of oscillation, i.e. the Strouhal number, is varied. For all the Strouhal numbers presented in Figure 4 the response of the membrane is rather sluggish initially. Furthermore, the response is rapid until the membrane convergence length reaches a maximum value. Beyond the maximum point the convergence length decreases rapidly to reach a shallow minimum. Thereafter the convergence length increases slowly to the steady state value corresponding to $C_{pn} = 0$ and the cycle repeats periodically with the same amplitude and period as that of the pressure coefficient. This behaviour is to be expected since the liquid membranes analysed in this paper are inviscid and there is no viscosity in the system to damp out the oscillations. It can be observed that the lag time between the maximum of the C_{pn}-curve and the corresponding maximum of the convergence length curve is more than the lag time between the minimum of the C_{pn}-curve and the minimum of the convergence length curve. It was seen in Part I that the response of membranes to decreasing pressure coefficients is quicker than the response to increasing pressure coefficients. The sharp drop in the convergence length and the

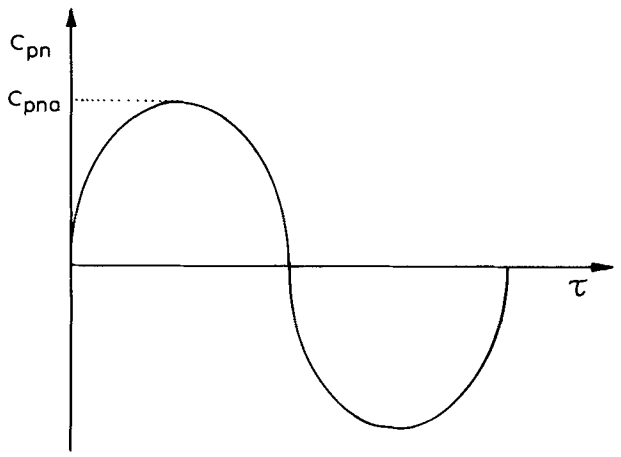

Figure 3. Schematic of a sinusoidal variation of the pressure coefficient C_{pn}

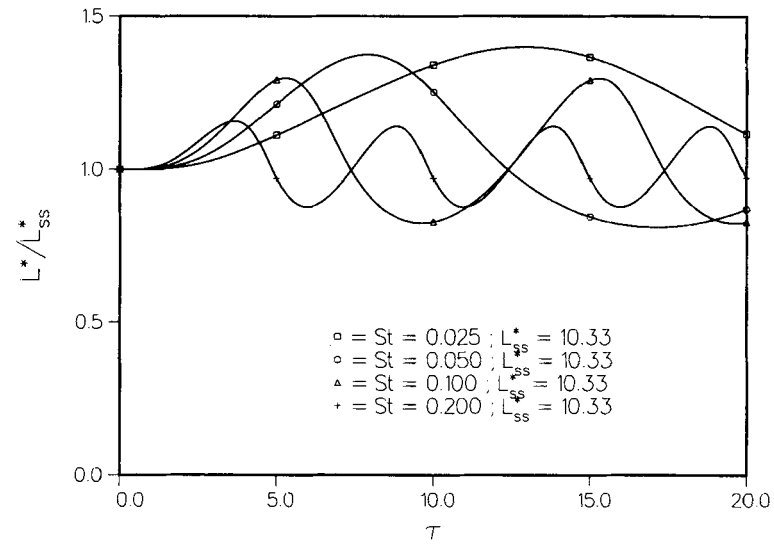

Figure 4. Normalized dimensionless convergence length as a function of the Strouhal number for a sinusoidal C_{pn}

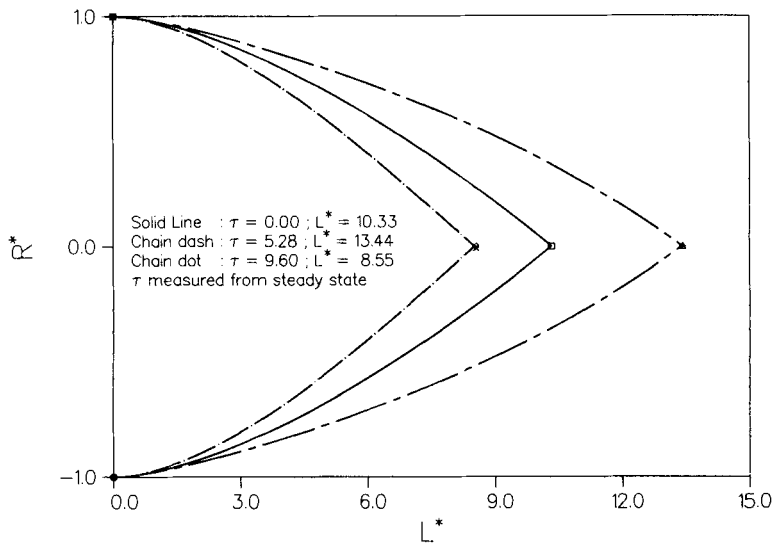

Figure 5. Membrane geometry at steady state (solid line), at the crest (dashed line) and at the trough (dashed–dotted line) of the response L^*/L^*_{ss} curve

non-identical crest lag time and trough lag time observed in Figure 4 can be attributed to this reason.[4]

The membrane profiles at steady state and at the extrema of the convergence length curve presented in Figure 4 are shown in Figure 5. Notice that the response for positive changes in C_{pn} is greater than for decreasing C_{pn}, in agreement with the results presented in Part I.

The dynamic response of the liquid membrane for several values of the Froude number, convergence parameter and nozzle exit angle is shown in Figures 6–8, respectively, where L_{ss}^* denotes the steady state convergence length corresponding to $C_{pn}=0$. In all these figures the Strouhal number and the amplitude of the pressure coefficient were kept constant. Figure 6 shows how the convergence length increases as the Froude number is increased. It can be seen from equation (36) that for a fixed Strouhal number (St) and other liquid membrane parameters, increasing the Froude number is equivalent to increasing the (non-dimensional) frequency of the imposed pressure fluctuations. As a consequence, the frequency of the convergence length oscillations increases as the Froude number is increased. The amplitude of the response curve, i.e. the peak value of the convergence length, decreases as the Froude number is increased. This implies that membranes with low Froude numbers are very sensitive to sinusoidally varying pressure coefficients, whereas membranes with higher Froude numbers are relatively more stable and can withstand higher amplitudes of oscillation of C_{pn}.

Figure 7 shows the dynamic response of the liquid membrane for several values of the convergence parameter. The effects of the liquid membrane inertia are clearly pronounced in this figure. High convergence parameters result in high inertia and hence near-zero amplitude, and the amplitude of the membrane oscillations increases as the convergence parameter decreases. In the limit $N \to \infty$, i.e. $\sigma \to 0$, the oscillation amplitude dies down to zero. Notice that the period of oscillation of the convergence length curve is the same for all three curves. This is attributed to the fact that the Strouhal and Froude numbers are fixed (see equation (36)).

The influence of the nozzle exit angle θ_0 on membranes subjected to sinusoidally varying C_{pn} is presented in Figure 8. Large angles at the nozzle exit result in membranes exposed to the pressure difference over a greater area. This is the reason for the faster response of liquid curtains with higher values of θ_0. The converse holds for curtains with small nozzle exit angles. Again, since the Strouhal number is kept fixed, the period of the response curves remains unaltered by changes in θ_0.

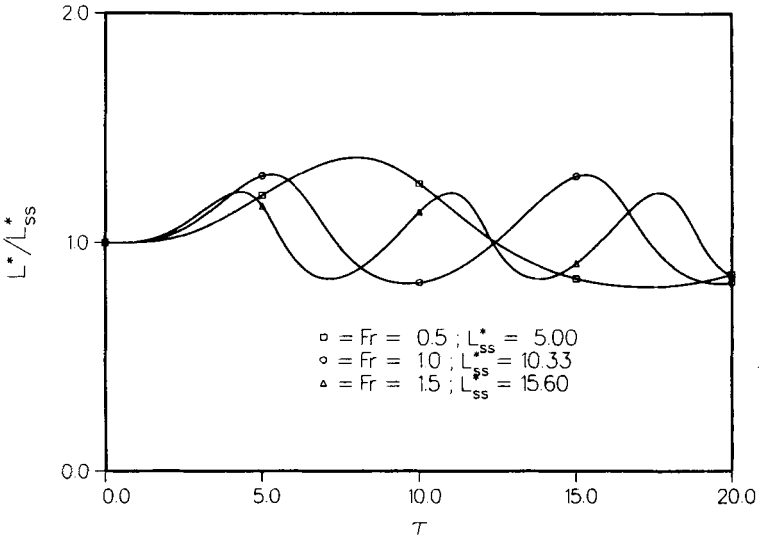

Figure 6. Normalized dimensionless convergence length as a function of the Froude number for a sinusoidal C_{pn}

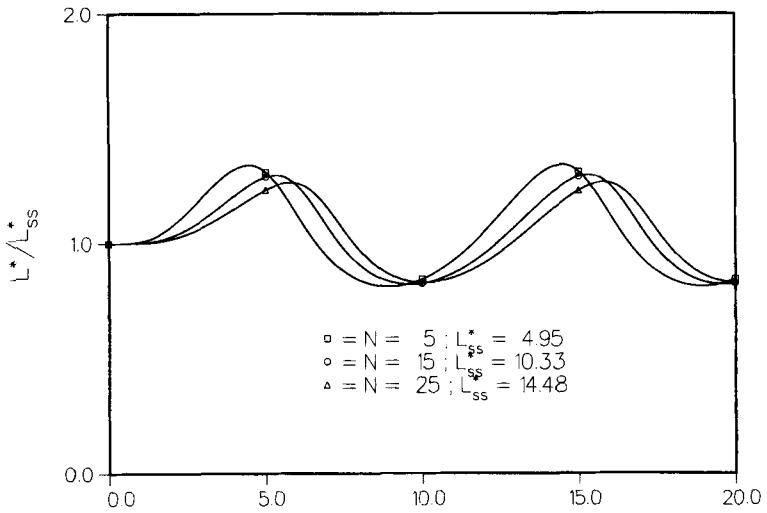

Figure 7. Normalized dimensionless convergence length as a function of the convergence parameter for a sinusoidal C_{pn}

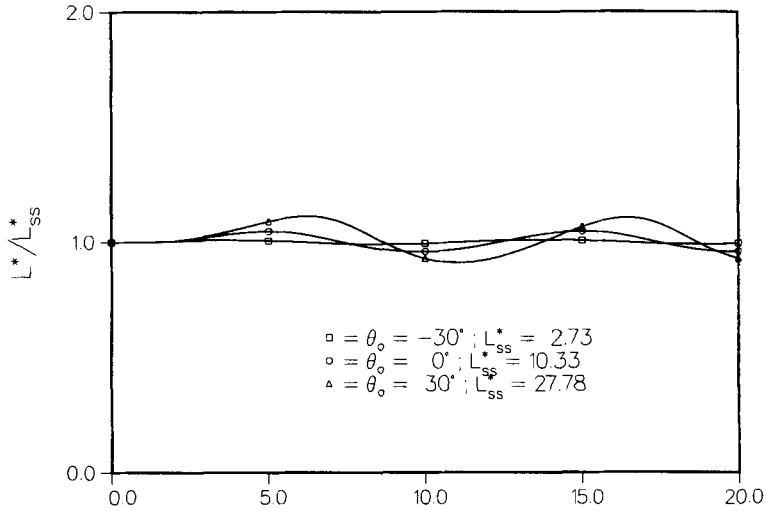

Figure 8. Normalized dimensionless convergence length as a function of the nozzle exit angle for a sinusoidal C_{pn}

Linear analyses[1] of steady state liquid curtains predict that for $\theta_0 = 0$ the critical pressure coefficient has a value of unity. For $C_{pn} < 1$ the membrane converges, while for $C_{pn} > 1$ the membrane diverges; and for $C_{pn} = 1$ an infinitely long cylindrical annular membrane is obtained. In Figure 9 the Strouhal number is fixed at 0·2 and the amplitude of the pressure coefficient is varied. Figure 9 indicates that the maximum value of the convergence length for the case of a sinusoidally fluctuating pressure coefficient is less than that of a membrane at steady state with pressure coefficient equal to C_{pna}. Figure 9 also shows that the peak value of the convergence length curve decreases as the Strouhal number (frequency) increases.

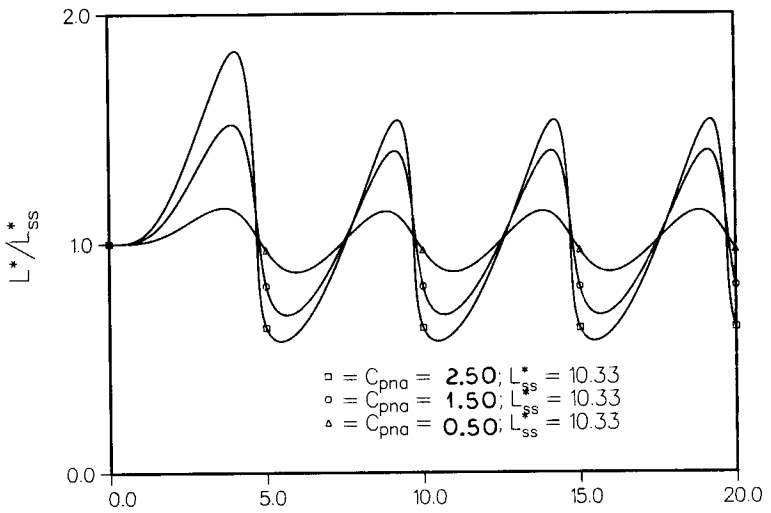

Figure 9. Normalized dimensionless convergence length as a function of C_{pna} for sinusoidal C_{pn}

The results shown in Figure 9 indicate that the oscillatory variation of the pressure coefficient coupled with the lagged response of the membrane results in the pressure coefficient 'felt' by the membrane always being less than C_{pna}. The extent to which the amplitude of the oscillating pressure coefficient is masked depends on the frequency of oscillation. The higher the frequency, the less is the effect of the pressure coefficient and the smaller is the peak of the convergence length curve. In the limit, as the Strouhal number tends to infinity, the peak tends to zero.

It can be seen from Figure 9 that the amplitude of the pressure coefficient could be as high as 2·5 times the critical value of unity determined from linear analyses[1] without affecting the stability of the membrane. Increasing the Strouhal number allows for the factor to be even higher than 2·5. In Figure 9 all the curves have the same period. This is expected since the period of oscillation (Strouhal and Froude numbers) of the pressure coefficient is fixed.

The results shown in Figures 2 and 4–9 were calculated using the two adaptive methods presented in this paper and with the non-adaptive technique presented in Part I. The calculations corresponding to Figures 4–9 were started from steady state liquid membranes with $C_{pn}=0$ and the pressure coefficient of equation (36) was imposed at $\tau=0^+$. The two adaptive methods presented in this paper yield almost indistinguishable results; the differences in convergence lengths were less than 0·05%, whereas the differences between the non-adaptive[1] and adaptive finite difference methods were at most 15%. Note, however, that the non-adaptive methods of Part I did not use all the grid points, as indicated below. The adaptive techniques presented in this paper required more computer time than the non-adaptive methods of Part I. This difference in computer times was due to the integrodifferential character of the adaptive finite difference methods presented in this paper (see equation (22)). Note that equation (22) is coupled with equations (12) and (25) and that the adaptive methods presented in this paper require the solution of equations (12) and (22) or equations (22) and (25), i.e. five differential equations, as compared with the solution of the four differential equations of the non-adaptive methods described in Part I. However, the adaptive methods of Part II use all the grid points in the calculations and adapt the grid to the temporal variations of the downstream boundary of the computational domain, i.e. to the convergence point, whereas the non-adaptive methods of Part I do not use all

the grid points if $L^*(\tau) < L^*_{max}$; these non-adaptive methods also require that L^*_{max} be known before transient calculations are performed.

The 15% difference between the results of the adaptive and non-adaptive methods can also be attributed to the fact that the adaptive methods use all the 300 or 400 grid points, whereas a lesser number of grid points was used by the non-adaptive techniques of Part I.

CONCLUSIONS

Two adaptive finite difference methods have been developed and applied to study the dynamic response of inviscid, incompressible, isothermal, axisymmetric liquid membranes subject to imposed sinusoidal pressure oscillations as a function of the Froude number, convergence parameter and nozzle exit angle. Both adaptive techniques map the time-dependent physical domain whose downstream boundary is unknown onto a fixed computational domain. This mapping results in a system of integrodifferential equations; their integrodifferential character is due to the dependence of the liquid membrane convergence length on the membrane mass.

The two adaptive methods have been solved by means of a block implicit iterative technique which employs upwind differences for the convection terms, and yield almost identical results. Comparisons between the adaptive methods presented in this paper and the non-adaptive techniques reported in Part I[1] indicate that the differences between the adaptive and non-adaptive methods are approximately 15%. These differences are due to the fact that the non-adaptive methods do not use all the grid points in the calculations. However, the adaptive methods require longer computational times than the non-adaptive techniques because they have to solve five non-linearly coupled integrodifferential equations as compared with the four equations of the non-adaptive methods, and use more grid points in the calculations.

It has been shown that the dynamic response of liquid membranes to imposed sinusoidal pressure fluctuations indicates that the critical value of the pressure coefficient determined from steady state linear analyses[2] can be exceeded if a periodic fluctuation of fairly high frequency is imposed on the pressure coefficient. For instance, if the Strouhal number is 0·2, for the values of the membrane parameters studied in this paper the amplitude of the pressure coefficient could be as high as 2·5 times the critical value of unity of the steady state linear analysis without altering the stability and convergence of liquid membranes. It was also shown that the amplitude of the membrane response decreases as the frequency (Strouhal number) of the C_{pn}-curve increases. Parametric studies involving the membrane parameters, namely the convergence parameter N, the nozzle exit angle θ_0 and the Froude number Fr, show that the membrane response is controlled by inertia. However, unlike the response to step and ramp changes in C_{pn} analysed in Part I, the response to sinusoidal fluctuations in C_{pn} does depend on the Froude number (see equation (36)).

ACKNOWLEDGEMENTS

This work was supported by the Office of Basic Energy Sciences, U.S. Department of Energy under Grant No. DE-FG02-86ER13597 with Dr. Oscar P. Manley as the technical monitor. This support is greatly appreciated. The author also wishes to acknowledge the support provided by CRAY Research, Inc. through a grant from the 1988 CRAY Research and Development Grant Program and by the Pittsburgh Supercomputing Center.

REFERENCES

1. J. I. Ramos and R. Pitchumani, 'Dynamics of liquid membranes. I: Non-adaptive finite difference methods'. *Int. j. numer. methods fluids*, **12**, 859–879 (1991).
2. J. I. Ramos, 'Liquid membranes: formulation and steady state analysis', *Report CO/89/4*, Department of Mechanical Engineering, Carnegie-Mellon University, Pittsburgh, PA, 1989.
3. G. E. Shilov, *Linear Algebra*, Dover, New York, 1977, pp. 112–113.
4. J. I. Ramos and R. Pitchumani, 'Unsteady response of liquid curtains to time-dependent pressure oscillations.' *Report CO/89/3*, Department of Mechanical Engineering, Carnegie-Mellon University, Pittsburgh, PA, 1989.